9-3-2005

Biophysics of cardiopulmonary resuscitation with periodic z-axis acceleration of abdominal compression at aortic resonant frequencies

Charles F. Babbs
Purdue University, babbs@purdue.edu

Biophysics of cardiopulmonary resuscitation with periodic z-axis acceleration or abdominal compression at aortic resonant frequencies

Charles F. Babbs[a,b]

[a] Department of Basic Medical Sciences, Purdue University; 1246 Lynn Hall, West Lafayette, IN 47907-1246, USA

[b] Indiana University School of Medicine, Indianapolis, IN, USA

Address for correspondence and proofs:
Charles F. Babbs, MD, PhD
1426 Lynn Hall
Purdue University
West Lafayette IN 47907-1246, USA
E-mail: babbs@purdue.edu
Voice: 765-496-2661, Fax: 765-494-0781

Draft September 3, 2005

Abstract

Periodic z-axis acceleration (pGz)-CPR involves oscillating motion of a whole patient in the head-to-foot dimension on a mechanized table. The method is able to sustain blood flow and long-term survival during and after prolonged cardiac arrest in anesthetized pigs. However, the exact mechanism by which circulation of blood is created has remained unknown. ***Objectives:*** To explain the hemodynamic mechanism of pGz-CPR and to suggest theoretically useful improvements. ***Method:*** Computer modeling using a hybrid analytical-numerical approach, based upon Newton's second law of motion for fluid columns in the aorta and vena cavae, Ohm's law for resistive flow through vascular beds, and a 10-compartment representation of the adult human circulation. This idealized 70 kg human model is exercised to explore the effects upon systemic perfusion pressure of whole body z-axis acceleration at frequencies ranging from 0.5 to 5 Hz. The results, in turn, suggested studies of abdominal compression at these frequencies. ***Results and conclusions:*** Blood motion induced in great vessels by periodic z-axis acceleration causes systemic perfusion when cardiac valves are competent. Blood flow is a strong function of the frequency of oscillation. Peak flow occurs in narrow frequency ranges. At 3.5 Hz, periodic acceleration using ± 0.6 G and ± 1.2 cm oscillations induces forward blood flow of 2.1 L/min and systemic perfusion pressure of 47 mmHg. A form of resonance occurs at the frequency for peak-flow, in which the period of oscillation matches the round-trip transit time for reflected pulse waves in the aorta. For ± 1.0 G acceleration at 3.5 Hz, systemic perfusion pressure is 80 mmHg and forward flow is 3.8 L/min in the adult human model with longitudinal z-axis motion of only ± 2 cm. Similar results can be obtained using abdominal compression to excite resonant pressure-volume waves in the aorta. For 20 mmHg abdominal pressure pulses at 3.8 Hz, systemic perfusion pressure is 71 mmHg and forward flow is 2.8 L/min. pGz-CPR and high frequency abdominal CPR are physically realistic means of generating artificial circulation during cardiac arrest. These techniques have fundamental mechanisms and practical features quite different from those of conventional CPR and the potential to generate superior systemic perfusion.

Key words: Abdominal, Aorta, Coronary perfusion pressure, Heart arrest, IAC-CPR, Inertia, pGz, Pulse wave velocity, Reflection, Resonance

---

Introduction

Periodic z-axis acceleration provides a novel method for resuscitation from cardiac arrest. The victim is placed lengthwise on an oscillating table. The table moves horizontally on nylon wheels in stainless steel tracks in the head-to-tail direction, referred to as the z-axis[1-4]. The amplitude of the oscillations is on the order of several centimeters, and the frequency of oscillations is typically 2 cycles per second. The resulting peak accelerations studied and reported so far[1-4] are approximately ± 0.6 G. (For reference, a person jumping up and down on the Earth's surface at a frequency of 1.5/sec to a total height of 20 cm generates peak accelerations of about ± 1 G.) In the literature this method is known as pGz-CPR, denoting periodic acceleration along the z-axis (Figure 1).

pGz-CPR is capable of maintaining the viability of anesthetized juvenile pigs in ventricular fibrillation for over 18 minutes[1]. After defibrillation, followed by a few cycles of conventional chest compression, the animals show consistent return of spontaneous circulation. Because 15 to 20 min of ventricular fibrillation is almost uniformly lethal without artificial circulation[5-7], such experiments demonstrate that pGz-CPR must be generating a form of artificial cardiac output, and in particular coronary perfusion. Moreover, the method leads to 48-hour survival with normal neurological function in experimental animals after 3 min of untreated ventricular fibrillation, followed by 15 min of pGz-CPR[3]. There is echocardiographic evidence of better stroke volume after resuscitation from prolonged cardiac arrest with pGz-CPR than with standard (Thumper) CPR, suggesting adequate coronary blood flow during pGz.

To date this method has suffered from the lack of any theoretical understanding of how artificial circulation can be generated by such z-axis giggling. A suitable theory would be helpful both for understanding the phenomenon and for optimizing flow, especially by specifying the best frequency of oscillation. In video recordings, pGz produces an obvious and vigorous sloshing motion of the abdominal contents from head to tail[3, 8], leading to the hypothesis that diaphragmatic motion may produce a degree of cardiac compression, as well as moderate ventilation[1]. An alternative hypothesis, not previously described, is that the motion of blood columns within the aorta and vena cavae themselves creates an "inertial pump" at particular frequencies of oscillation. Such an inertial pump could be activated by means other that whole body acceleration. One practical choice, given the stiffness of the rib cage, is abdominal compression at higher frequencies than those previously studied. The objective of the present investigation is to explore in detail the biomechanics and hemodynamic consequences of these alternative mechanisms.

Methods

Approach

A person standing in a rising elevator feels a tug of artifical gravity as the elevator accelerates upward. Within the internal frame of reference of the elevator the passenger experiences acceleration toward the floor of the elevator that is equal and opposite to the upward acceleration of the elevator in the shaft[9]. Acceleration of this local frame of reference produces artificial gravity, which by all possible experiments conducted within the elevator is indistinguishable from ordinary gravity. Similarly, acceleration of the whole body along its longitudinal axis, as shown in Figure 1, produces artificial gravity acting on the freely moving abdominal contents and diaphragm, relative to the pelvis, rib cage and spine, causing secondary changes in intrathoracic volume. The same artificial gravity also induces motion of the blood columns in the aorta and vena cava with respect to the walls of these great vessels. In this case the walls of the vessels are analogous to the walls of the elevator, and the blood is analogous to a passenger in the elevator.

To examine in detail how periodic acceleration of the whole body induces motion of blood in the circulatory system, one can envision as a first approximation the model sketched in Figure 2, in which 4 aortic segments and 4 caval segments are aligned with the z-axis of acceleration. Here the z-axis is horizontal. The lumped right heart and left heart compliances include the right ventricle and pulmonary arteries (C_{rh}) connected in series with the left ventricle and pulmonary veins (C_{lh}). Critical one-way valves (tricuspid and aortic) direct flow from veins to arteries through the lungs. The compliances C_{rh} and C_{lh} are subjected to generalized intrathoracic pressure, which changes as the diaphragm and abdominal contents move relative to the rib cage and spine along the z-axis, and also as air flows in and out through the trachea. The physical properties of the system are listed in Table 1. In this system one possible mechanism generating blood flow is the bellows-like movement of the diaphragm[3, 8]. A second, less obvious mechanism is the motion of blood columns within the aorta and vena cavae. Let us begin with phrenic motion.

Motion of the diaphragm

From a mechanical viewpoint the lungs can be regarded as gas filled balloons open to air via the tracheobronchial tree. Let P_{lung} represent pressure in the lungs or generalized intrathoracic pressure. Let P_{mouth} represent pressure at the mouth, which could be either zero atmospheric pressure or forced inspiratory pressure in the case of controlled ventilation. Let C_{lung} represent lung-chest compliance, and let R_{airway} represent airway resistance.

Lung pressure compared to atmospheric pressure is $P_{lung} = (\Delta V_{chest} + V_{in} - V_{out})/C_{lung}$, where ΔV_{chest} is the change in lung volume do to motion of the diaphragm in pGz-CPR, $V_{in} - V_{out}$ is the net volume change via the open airways, and C_{lung} is the combined lung-chest wall compliance. Here for simplicity we do not include changes in blood volume

within the thorax, which are small compared to volume changes caused by motion of the diaphragm.

The change in lung pressure over a small time interval dt may be given by the expression

$$dP_{lung} = \frac{dt}{C_{lung}}\left[\dot{z}_D A_D - \frac{\left(P_{lung} - P_{mouth}\right)}{R_{airway}}\right]. \qquad (1)$$

Here $\dot{z}_D$ is the rate of z-axis movement of the diaphragm toward the head, A_D is the cross sectional area of the diaphragm (~400 cm^2). The left hand term, $\dot{z}_D A_D$, is the rate at which thoracic volume is changed by movement of the diaphragm. The right hand term is the flow of gas out of the chest via the airways through the airway resistance. Equation (1) gives the corresponding pressure change, assuming that the volume changes are small with respect to total lung volume.

Owing to the suspension of the stomach and intestines on mesenteric stalks, the embryonic development of the liver, and the presence of the lubricating peritoneal cavity, the abdominal contents are essentially free-floating with respect to the walls of the peritoneal cavity. The relatively massive liver, stomach, and intestines are the passengers in the elevator and the abdominal walls and retroperitoneal space, braced by the ribs, pelvis, and spine, are the walls of the elevator. The diaphragm moves with the abdominal contents.

For periodic sinusoidal acceleration of the abdominal contents and diaphragm along the z-axis, we have

$$z = B\sin(\omega t) \qquad (2a)$$

$$\dot{z} = B\omega\cos(\omega t) \qquad (2b)$$

$$\ddot{z} = -B\omega^2\sin(\omega t) \qquad (2c)$$

for phrenic displacement, z, toward the head, velocity of displacement $\dot{z}$, and acceleration $\ddot{z}$. (Here the "dot" over z indicates the first time derivative, and the “double dot” over z indicates the second time derivative.) The constant B represents the maximal amplitude of oscillations in meters or centimeters relative to the starting position of the patient. The peak-to-peak or total distance moved is twice B. Sin(ωt) and cos(ωt) represent the sine and cosine functions, and $\omega = 2\pi f$ is the angular frequency of oscillation for periodic motion at frequency, f. Equations (2a), (2b), and (2c) are obtained by successive differentiation of the sine function for ordinary periodic motion. They hold as long as the diaphragm remains relatively loose and freely moving.

The vigor of pGz-CPR is usually specified in terms of the peak amplitude of acceleration in either direction, which is $B\omega^2$, measured in Gs or multiples of the gravitational

acceleration of a mass at the Earth's surface. If we take this peak value $G_{max} = B\omega^2$, as a given parameter describing the vigor of oscillation, then by substituting equation (2b) into equation (1) we can express the change in thoracic pressure as a result of diaphragmatic motion as

$$dP_{lung} = \frac{dt}{C_{lung}}\left[-A_D \frac{G_{max}}{\omega}\cos(\omega t) - \frac{\left(P_{lung} - P_{mouth}\right)}{R_{airway}} \right]. \qquad (3a)$$

(It is important to establish the convention that motion of the pGz-CPR platform begins at time zero with headward motion of the whole body. In this case the velocity of the diaphragm is negative in sign, toward the feet, at time zero.) In turn, the prevailing intrathoracic pressure that squeezes the cardiac chambers and pulmonary vessels at any time, t , can be determined numerically in a computer model, given the initial conditions and the known parameters of the system, by computing

$$P_{lung} = \int_0^t dP_{lung} . \qquad (3b)$$

This cyclic pressure in the lungs is one possible mechanism for generating blood flow in pGz-CPR. The fluctuations in lung pressures are applied to the right and left heart compliances in Figure 2. They are analogous to those created by gasping or agonal respirations during early cardiac arrest, and can perhaps serve to sustain some degree of perfusion[10, 11]. We may refer to this mechanism as the bellows pump.

Upon reflection, however, there is another mechanism that can generate blood flow during pGz-CPR, and this is the acceleration of blood itself along the long axes of the aorta and vena cavae. The blood columns within the aorta and vena cavae feel oscillating craniocaudal tugs, which cause them to move with respect to the walls of their containers. This inertial mechanism turns out to be the more powerful of the two.

Motion of aortocaval blood columns

In the simplified model of Figure 2 the vena cavae and aorta are regarded as a series of straight, blood filled tubes, divided into segments numbered 1, 2, 3, and 4. The two ends of the aorta and of the vena cavae are closed, and systemic perfusion occurs via side branches. Let Q_k indicate axial flow exiting the right hand (caudal) end of segment k, moving toward the feet, as shown in Figure 3. Let P indicate the blood pressure at the midpoint of each segment, A the cross sectional area of each segment, r its radius, and V its volume. The cross sections of the segments are circular. Variables V, Q, A, r, and P are functions of time, owing to the bulk flow of blood between segments. These variables are defined at the mid point of each segment. For simplicity, let us assume the aortocaval segments have equal length (about one quarter of truncal length), denoted as constant $\Delta L \approx$ 12 cm for an adult human. Segments 1 and 4 include longitudinal blood volumes in the

carotid, jugular, and iliac vessels, which are regarded functionally as extensions of the aorta and vena cavae in the z-dimension.

The rate of change in the volume of aortocaval segment k is the difference between flow in and flow out, that is

$$dV_k / dt = Q_{in} - Q_{out} = Q_{k-1} - Q_k . \qquad (4)$$

Q_k is defined as the discharge of blood from the right-hand (caudal) end of each segment. This is the first governing equation for the system.

Now imagine a slug or column blood traveling from segment k to segment k+1 moving toward the feet and having length ΔL and a diameter equal to that of the smaller of the two adjoining segments. Let

$$A'_k = \min(A_k, A_{k+1})$$

represent the cross sectional area of this blood column. To find the second governing equation for flow, we must account for the force required to overcome inertia of the slug. The inertial force is given by Newton's second law, force = mass x acceleration, or

$$F_{Ik} = \rho \Delta L A'_k \frac{d(Q_k / A'_k)}{dt},$$

where Q_k / A'_k is the velocity of the blood column (assumed to be uniform over the cross section), and ρ is constant blood density. Flow Q_k is positive in sign when it leaves the "right hand" end of segment k and enters the "left hand" end of segment k + 1, moving toward the feet.

The force overcoming resistance to fluid flow between the mid point of segment k and the mid point of segment $k+1$ is much less than the inertial force for these large vessels; however for completeness it may be estimated as the force required to drive flow Q_k through a tube of length ΔL and cross section A'_k. Using "Ohm's Law", force/area = flow x resistance, together with Poiseuille's Law,

$$\text{resistance} = \frac{8}{\pi} \cdot \frac{\text{viscosity} \cdot \text{length}}{\text{radius}^4} = 8\pi \cdot \frac{\text{viscosity} \cdot \text{length}}{\text{area}^2} = 8\pi \cdot \frac{\nu \Delta L}{A'^2},$$

we have the force needed to overcome viscous resistance, namely area x flow x resistance,

$$F_{Rk} = A'_k Q_k \left(8\pi \cdot \frac{\nu \Delta L}{A'^2} \right) = 8\pi \nu \Delta L \cdot \frac{Q_k}{A'} .$$

The total force driving the column of blood through the one half of segment k and one half of segment $k+1$ is provided by the difference in pressure between the two ends of the slug, multiplied by A'_k, plus in simulations of pGz-CPR the weight of the slug under time-varying acceleration, g, along the z-axis, namely

$$F_{Ik} + F_{Rk} = P_k A'_k - P_{k+1} A'_k + g\rho\Delta L A'_k .$$

Here internal acceleration, g, is positive in sign when blood moves toward the feet. In this case the whole body moves headward. Thus $g = +B\omega^2 \sin(\omega t)$.

So, we have the balance of forces

$$F_{Ik} + F_{Rk} = \left(P_k - P_{k+1} + g\rho\Delta L\right)A'_k = +\ \rho\Delta L A'_k \frac{d(Q_k / A'_k)}{dt} + \frac{8\pi\nu\Delta L Q_k}{A'_k},$$

or

$$\frac{d(Q_k / A'_k)}{dt} = \frac{P_k - P_{k+1}}{\rho\Delta L} + g - \frac{8\pi\nu}{\rho} \cdot \frac{Q_k}{\left(A'_k\right)^2} . \qquad (5)$$

The rightmost term in equation (5), containing blood viscosity, ν, is the small correction for aortocaval resistance.

Equations (4) and (5) describe in relatively simple mathematical form the flow, pressure, and expansion (change in area or volume) in each of the aortocaval segments of the model under periodic z-axis acceleration. They can be solved numerically, using the methods in Appendix 1, to describe sloshing of blood back and forth in these great vessels. In addition, Ohm's Law can be used to calculate resistive flow through systemic vascular beds from the aortic to the caval side and back again through the right heart, lungs, pulmonary blood vessels, and left heart, as indicated in Figure 2. Ohm's Law, which relates flow to pressure and resistance, is $i = (P_1 - P_2)/R$, where $P_1 - P_2$ is the instantaneous difference in pressure across resistance R as flow i occurs. In this way the movement of blood in the model can be described in the presence of full cardiac arrest and periodic z-axis acceleration of the whole body, or alternatively, periodic compression of the aorta and vena cava through the soft abdominal wall.

Initial conditions. Input parameters for the numerical calculations are provided in Table 1. Anatomic and physiologic parameters describing an idealized normal "70 Kg man"[12] are used to specify values of the compliances and resistances of the vascular compartments, as described in detail previously[13]. Further details of the rationale for selection of resistance and compliance values are provided in references[12, 14, 15].

The model was solved using Microsoft Visual Basic Macros within a Microsoft Excel spreadsheet to perform numerical integration using equations (6c) through (12) in

Appendix 1. The initial conditions included mean circulatory pressure of 10 mmHg in all vascular compartments, resting aortic radius 1.0 cm in segments 1 through 4, and resting caval radius 1.5 cm in segments 1 through 4. For convenience and accuracy, all variables were converted to units of meters, kilograms, and seconds prior to calculation. The model was driven either by internal sinusoidal acceleration $g(t) = G_{max} \sin(\omega t)$ for various peak accelerations, G_{max}, and angular frequencies, ω, or by external positive pressure $P_{ext}(t) = \frac{P_{max}}{2}\left(1 - \cos(\omega t)\right)$ applied to both aortic and caval segments 3 and 4 to simulate abdominal compression. Results are expressed in terms of mean systemic perfusion pressure ($P_{2a} - P_{2v}$) in mmHg or forward flow ($i_1 + i_3 + i_4$) in L/min. Tracheal airflow is also calculated as $\left(P_{mouth} - P_{lung}\right)/R_{airway}$.

Numerical accuracy. The accuracy of the numerical solution was verified by computing conservation of volume routinely, by comparing pulse wave velocity with the analytical result of the Moens-Korteweg equation (Appendix 2), and by computing conservation of energy for resonant pulse waves in the aorta for no-leak test cases with extremely high peripheral vascular resistance.

Making movies. To illustrate motion of blood columns within the aorta and vena cavae the radii of the 4 aortic and 4 caval segments were displayed automatically as a function of time using Visual Microsoft Visual Basic macros to manipulate graphics objects. Animated aortocaval cylinders are shown in longitudinal cross section. Freeze frame pictures may be obtained by stopping the animation at particular times to illustrate patterns of blood movement that generate systemic perfusion pressure. This method proved especially effective at elucidating the mechanism of pGz-CPR and resonant motion of blood within the aorta. An electronic copy of the Excel spreadsheet containing the movie macros is available from the author (babbs@purdue.edu) upon request.

Results

Mechanism of pGz-CPR

Because results are highly frequency dependent, it is best to begin with plots of systemic perfusion pressure vs. frequency of oscillation. Figure 4(a) illustrates such frequency spectra for periodic z-axis acceleration under 4 conditions: bellows pump only, inertial pump only, both, and neither. In Figure 4(a) the peak acceleration was fixed for all frequencies at ± 0.6 G, as described in the papers of Adams et al[1, 3]. When only the bellows pump mechanism is enabled in the model, lung pressures fluctuate as described in Equation (3) as the diaphragm and abdominal contents move with respect to the rib cage. Fluctuations in intrathoracic pressure create forward flow and perfusion pressures, but only to a biologically meaningful extent at frequencies below 1 Hz. Moreover, at 0.5 Hz or 30 cycles/min, the amplitude of excursion of the whole patient must be ± 60 cm, that is a total travel of 120 cm, in order to achieve ± 0.6 G peak acceleration. Clearly, ± 60 cm motion of the diaphragm with respect to the rib cage is not possible anatomically. Thus, to

generate even modest blood flow, the bellows pump must exceed practical limits. Although the bellows pump can produce some ventilation (about 50 ml tidal volume in this model at 3.5 Hz), it does not explain the generation of blood flow during pGz-CPR at frequencies of 2 Hz and greater.

When only the inertial pump mechanism is enabled in the model, blood is impelled to oscillate in the aorta and vena cavae without changes in lung volume or pressure. As shown in Figure 4(a), this mechanism can produce biologically meaningful perfusion pressures at certain frequencies above 1 Hz. The effect is highly frequency dependent, however. In the model of Figure 4(a), the best perfusion pressure occurs at between 3 and 4 Hz. Thus the inertial pump involving acceleration of aortocaval blood columns is the more likely mechanism of pGz-CPR. Figure 4(b) gives a survey of the effects of varying peak accelerations. Systemic perfusion pressure is directly proportional to the peak amplitude of whole body acceleration. The frequency for best systemic perfusion is independent of the amplitude of z-axis acceleration.

Pressure-volume waves in space and time

To explore what is happening near peak flow frequencies it is helpful to study computer animations of aortic and caval wall motions. Still frames of a typical animation sequence shown in Figure 5 reveal that the model of Figure 4 (with inertial pump only) produces some rather remarkable behavior when subjected to periodic z-axis acceleration at 3.75 Hz with z-axis motion ± 1.2 cm and ± 0.6 G acceleration. There is a definite sloshing of blood back and forth along the z-axes of the aorta and vena cavae, which is much more prominent on the aortic side. In Figure 5 diameters of the aorta (above) and vena cavae (below) are drawn to scale. Balls indicate fluid markers at the 20^{th}, 40^{th}, 60^{th} and 80^{th} percentiles of volume along the z-axes. These markers allow one to track fluid motion, just as do smoke streams in a wind tunnel or fallen leaves on the surface of a stream. The markers show that the blood in the aorta sloshes first toward the head and then toward the tail during pGz, relative to blood in the cavae, which moves a much smaller distance. Dotted lines indicate resting, zero-G diameters of the great vessels.

As is evident from the animations, the velocity of blood motion and the extent of travel of along the z-axis are much greater in the aorta than in the cava at 3.75 Hz. Reference to the dashed lines, showing the initial outlines of the great vessels, shows that waves of expansion and contraction, sometimes called inflation waves, traverse the great vessels at the driving frequency. There is partial collapse of the caudal aorta during headward motion of the blood column (Figure 5(a)). There is similar collapse of the cranial aorta when the majority of intra-aortic blood volume moves toward the feet (Figure 5(b)). During these periods of collapse there is low pressure in the involved aortic segments, and consequently a small amount of retrograde flow occurs in the head and legs (data not shown).

As pressure-volume waves traverse segments 2v and 2a, they influence the pressure gradients across the tricuspid and aortic valves. When peaks pass by the tricuspid valve on

the venous side they allow for valve opening and forward flow into the right heart. When troughs pass the aortic valve on the arterial side they allow aortic valve opening and forward flow into the aorta. Flows across the aortic and tricuspid valves in the model are shown in Figure 6 for the peak-flow frequency. Elimination of tricuspid and aortic valve function diminishes positive mean systemic perfusion pressure in the model to less than 2 percent of the values obtained with competent valves. Thus competent heart valves are critical for the function of the inertial pump.

Aortic resonant frequencies

The animations of aortic wall motion shown in Figure 5 suggest a form of resonance. In particular, the peak-flow frequencies seem related to the round-trip pulse transit times for the length of the aorta. Consider a thin walled elastic tube of length, L, and initial radius, r_0, and cross section A_0. The compliance of the tube is C and the density of fluid within it is ρ. As shown in Appendix 2, it is possible to estimate the round-trip pulse transit time for the aorta in terms of the parameters of our models by combining the classical Moens-Korteweg equation for the pulse wave speed in a thin walled tube and the formula for compliance of such a tube to give

$$t_{rt} = 2\sqrt{\frac{LC\rho\left(1+\Delta r/r_0\right)}{A_0}}.$$

For small volume pulses with small changes in radius ($\Delta r/r_0 \approx 0$) we can calculate the frequency for reflected pulse waves making one complete round trip up and down the aorta as

$$f^* = \frac{1}{t_{rt}} \approx \frac{1}{2}\sqrt{\frac{A_0}{LC\rho}}.$$

The round trip frequency, f*, for the parameters of Figure 4 is 3.6 Hz. This value matches the peak frequency of 3.5 Hz in Figure 4. In this case the blood in the aorta would receive an impulsive push just as the reflected pulse wave arrives at its starting point, and so the pulse would be amplified on successive cycles, rather like a parent pushing a child on a playground swing.

At resonant frequency excitation, the total systemic flow in this adult human model can be rather remarkable, about half of the normal 5 L/min cardiac output in an idealized 70 kg man. In the particular example of Figure 7 (± 0.6 G, ± 1.2 cm oscillations) net forward flow is 2.8 L/min over the interval from 20 to 24 seconds. Average forward flow is 1.9 L/min in this model over the interval from 20 to 50 sec, with both bellows and inertial pumps working. Instantaneous pressures and flows vary considerably in a quasi-random fashion over time. Thoracic arterial and venous pressure waveforms are shown in Figure 7. Large irregular arterial pulses drive forward flow. These aortic pressure waves resemble the electrocardiographic waves of ventricular fibrillation (Figure 7(a)) and are

similar in shape and in range to those reported by Adams[4] for animal studies in older pigs. Venous pressures remain low because the veins are off their resonant frequency when the aorta is on resonance, owing to the compliance differences between veins and arteries. The irregular pattern of arterial pressure does change over time, but positive perfusion pressure is sustained indefinitely (Figure 7(b)). The detailed structure of the pressure fluctuations in Figure 7(b) with pGz at 3.5 Hz is clearly different from the detailed structure with 3.4 Hz or with 3.6 Hz (data not shown). However, the general pattern is similar. When the frequency of excitation is off resonance, the amplitudes of the arterial and venous pressures are much more similar, and the systemic perfusion pressure falls to less than 10 mmHg.

Perfusion pressure at any chosen frequency is proportional to the peak acceleration (Figure 4(b)) and can be further augmented for accelerations greater than ± 0.6 G. For example, at ± 1.0 G systemic perfusion pressure for the adult human model is 80 mmHg and flow is 3.8 L/min. For reference, conscious human subjects subjected to ± 0.4 G peak acceleration in the z-axis find the experience uncomfortable but tolerable[16]. However, repeated z-axis accelerations of 5 to 6 Gs are considered adequate to cause rupture of the aorta[17].

High frequency abdominal compression

An alternative way to induce resonant fluid waves in the aorta is by application of external pressure. In Figure 8 we see the results of the application of sinusoidal abdominal pressure ranging from zero to +10, +20, or +30 mmHg at frequencies ranging from 1 to 5 Hz. High frequency abdominal compressions produce resonant oscillations in the aorta similar to those produced by periodic z-axis acceleration. Thoracic arterial and venous pressure waveforms are similar to those shown in Figure 7. In these simulations of abdominal compression, the compliance of that abdominal aorta was tapered. Experimentally, the compliance of the abdominal aorta is less than that of the thoracic aorta[18]. Since the results might have been biased in a positive direction by assuming average rather than below average values for abdominal aortic compliance, a linear tapering function for the axial change in aortic compliance was used, multiplying average aortic compliance by the constants T1, T2, T3, and T4, equal respectively to 1.6, 1.2, 0.8, and 0.4. Thus mid abdominal aortic compliance was half that of mid thoracic aortic compliance, in keeping with published experimental data[18]. Nevertheless, a strong resonance developed in the aorta. In the case of abdominal pressure forcing at 3.8 Hz, shown in Figure 8 for 20 mmHg positive abdominal pressure pulses, net forward flow is 2.8 L/min over the interval from 20 to 50 seconds. For zero to 30 mmHg abdominal pressure pulses at 3.8 Hz, forward flow is 3.4 L/min in this adult human model.

Discussion

In his classic essay on the early history of resuscitation[19], Hugh Stephenson, describes the medieval practice of equine CPR. The victim is laid across the back of a horse, which is made to trot around in a circle, providing a giggling motion at a frequency of a few cycles per second. Perhaps the oscillating table of pGz-CPR is the modern equivalent of the

horse. Perhaps manual or mechanical abdominal compression at the proper frequency can have the same effect with less patient motion.

The present theoretical investigation was motivated by the question of how pGz-CPR works. This question is especially appropriate to address with mathematical models. Hemodynamic data from animal models of pGz-CPR are scarce. Direct measurements of blood pressure and blood flow are prone to artifacts in vibrating subjects. High blood flow happens only in narrow peaks in the frequency domain, which would be easy to miss in any particular animal experiment or clinical trial, unless a large number of frequencies were tested routinely. Mathematical analysis, however, shows easily that periodic z-axis acceleration at certain frequencies in the range of 1 to 5 Hz can generate oscillating waves of blood volume and blood pressure within the aorta. Systemic perfusion is prominent when the cycle length of sinusoidal z-axis acceleration matches the round trip transit time for reflected pulse waves, such that a single zone of inflation moves up and down the aorta and is reinforced with each succeeding push (Figure 5).

In this case a type of resonance is established that multiplies aortic pressure and promotes systemic flow. Resonant frequencies for the aorta do not induce resonance in the vena cavae, because the compliances of large arteries and large veins are different. Thus substantial pressure differences can develop between the systemic arteries and systemic veins, inducing forward flow of blood (Figure 7). Competent heart valves help recycle blood from the venous side back to the arterial side through the lungs, so that the process can be sustained indefinitely. We refer to this general mechanism as the inertial pump, which is physically quite different from the better known cardiac pump, thoracic pump, and abdominal pump mechanisms of CPR[14, 20, 21].

In a resonating mass-and-spring system the energy imparted to the mass from one push is temporarily stored in the spring as potential energy. This stored energy is converted to kinetic energy and back again to potential energy, just in time to sum with that of the next push. A parent pushing a child on a playground swing is another example of such a system. When the period between pushes matches the round trip time for the swing, then the pushing is most effective and efficient. This additive effect of many pushes causes motion much greater than any single push could. In the pGz-CPR system the mass is the blood in the aorta, and the spring, or energy storage device, is the compliance of the aorta at either end. Blood is forced into one end, stretching the springs of the system, which are the elastic fibers of aorta at that end. (Microscopically the elastic fibers of the aorta look like little springs!) These fibers store energy and return it as a reflected pulse wave.

When the period of z-axis acceleration is equal to the round trip pulse transit time along the aorta, the effects of sequential pushes add and resonance happens (Figure 5). An irregular pattern of aortic pressure develops in part because there are partial reflections at the interfaces between segments, as well as at the ends, and because the driving frequency is slightly different from the primary resonant frequency based upon total aortic length. For such resonating systems, it is not especially important how energy is imparted to the system, as long as it is added at or near the resonant frequency. Thus abdominal compression at or near the aortic resonant frequency is quite effective at generating blood

flow in this theoretical model. Experimenters are encouraged to confirm or deny this result, keeping in mind that the exact resonant frequency may differ from model to model and from individual to individual.

The effectiveness of inertial pump CPR is indeed highly dependent upon the frequency of oscillations. Although the peak for resonance is narrow and may be hard to find, it is worth searching for, because ample blood flow can be obtained. If the method were implemented by a machine, the frequency and amplitude of oscillations could be tightly controlled. A mechanical resuscitation system incorporating a blood flow sensor, such as an end-tidal CO_2 monitor, could use feedback to adjust the oscillation frequency to resonance. (Note that controlled mechanical ventilation through an endotracheal tube would be needed for end-tidal CO_2 monitoring, as opposed to the gas exchange produced by pGz itself.) The force or pressure of each individual push could be small and essentially harmless, as suggested in Figure 8, when the pushes are delivered at the proper frequency. A less technically sophisticated and more clinical approach to feedback control might involve tuning the optimal frequency by observing the color of the patient, capillary refill in the forehead, constriction of the pupils, or a maximal palpable arterial pulse.

Using the Moens-Korteweg equation as a guide, one would predict that the optimal frequency is directly proportional to the square root of aortic stiffness (Young's modulus) and inversely proportional to aortic length. Thus peak flow frequencies may well be higher in older individuals with arthrosclerosis and also in children with shorter aortas. Adams' original discovery of apparent resonant frequency pGz-CPR in young laboratory pigs near 2 Hz rather than near 3.5 Hz in the adult models of the present paper may be related to much greater aortic compliance in these young food animals. Because of the strong frequency dependence of aortic resonance, the predictions of the present model may not match particular experimental results at any single frequency. However, the phenomenon of aortic resonance should remain, with the location of peak flow frequencies being determined by a balance of factors, including those in the Moens-Korteweg equation. This equation helps make clear what would otherwise be a complex mystery: high flows in some models and low flows in other, quite similar models.

Inertial pump CPR has some interesting practical features compared to conventional CPR. It is unlikely to cause rib fractures, liver laceration, or pulmonary contusion. If the inertial pump were implemented by abdominal pumping, both ventilation and electrical ventricular defibrillation could be easily accomplished without interruption of CPR. Inertial pump CPR may be especially appropriate for victims with multiple broken ribs, recent chest surgery, flail chest, or other conditions in which conventional chest compressions are especially hazardous or ineffective. In vivo, there is evidence that nitric oxide is released from endothelial cells preferentially in response to pGz (without cardiac arrest)[2] leading to reduced peripheral vascular resistance and greater flow for a given perfusion pressure[1]. Thus inertial pump-CPR offers a fresh new approach to the temporary management of cardiac arrest. Understanding of the underlying physics of aortic resonance can provide helpful insights and strategies for optimizing systemic blood flow, and in turn, resuscitation success.

References

1. Adams JA, Mangino MJ, Bassuk J, Kurlansky P, Sackner MA. Novel CPR with periodic Gz acceleration. Resuscitation 2001; 51:55-62.
2. Adams JA, Mangino MJ, Bassuk J, Kurlansky P, Sackner MA. Regional blood flow during periodic acceleration. Crit Care Med 2001; 29:1983-8.
3. Adams JA, Bassuk J, Wu D, Kurlansky P. Survival and normal neurological outcome after CPR with periodic Gz acceleration and vasopressin. Resuscitation 2003; 56:215-21.
4. Adams JA, Wu D, Bassuk J, Kurlansky P. Cardiopulmonary resuscitation (CPR) using periodic acceleration (pGz) in an older porcine model of ventricular fibrillation. Resuscitation 2004; 60:327-34.
5. Kern KB, Sanders AB, Badylak SF, et al. Long-term survival with open-chest cardiac massage after ineffective closed-chest compression in a canine preparation, Circulation 75, 1987.
6. Kern KB, Ewy GA, Voorhees WD, Babbs CF, Tacker WA. Myocardial perfusion pressure: a predictor of 24-hour survival during prolonged cardiac arrest in dogs. Resuscitation 1988; 16:241-250.
7. Eisenberg MS, Hallstrom A. Long term survival after out-of-hospital cardiac arrest. New England Journal of Medicine 1982; 306:1340-1343.
8. Adams JA, Mangino MJ, Bassuk J, Inman DM, Sackner MA. Noninvasive motion ventilation (NIMV): a novel approach to ventilatory support. J Appl Physiol 2000; 89:2438-46.
9. Paris A. Subtle is the Lord -- The Science and the Life of Albert Einstein. Oxford and New York: Oxford University Press, 1882:552.
10. Saiki C, Ikeda M, Nishikawa T, Tanimoto T, Yoshida S, Matsumoto S. The process of cardiorespiratory autoresuscitation in intact newborn rats. Can J Physiol Pharmacol 2001; 79:1036-43.
11. Sanocka UM, Donnelly DF, Haddad GG. Autoresuscitation: a survival mechanism in piglets. J Appl Physiol 1992; 73:749-53.
12. Hamilton(Section-Editor) WF, Dow(Executive-Editor) P. Handbook of Physiology Volume 2, Section 2: Circulation: American Physiological Society, Washington D.C., 1963:93-95.
13. Babbs CF. CPR techniques that combine chest and abdominal compression and decompression : Hemodynamic insights from a spreadsheet model. Circulation 1999; 100:2146-2152.
14. Babbs CF, Weaver JC, Ralston SH, Geddes LA. Cardiac, thoracic, and abdominal pump mechanisms in cardiopulmonary resuscitation: studies in an electrical model of the circulation. Am J Emerg Med 1984; 2:299-308.
15. Babbs CF, Ralston SH, Geddes LA. Theoretical advantages of abdominal counterpulsation in CPR as demonstrated in a simple electrical model of the circulation. Annals of Emergency Medicine 1984; 13:660-671.
16. Shoenberger RW. Discomfort judgements of translational and angular whole-body vibrations. Aviat Space Environ Med 1982; 53:454-7.

17. McCormack PD. Prediction of arterial wall failure under acceleration stress in high-performance aircraft. Aviat Space Environ Med 1984; 55:620-31.
18. Silver FH, Christiansen DL, Buntin CM. Mechanical properties of the aorta: a review. Crit Rev Biomed Eng 1989; 17:323-58.
19. Stephenson HE. Historical views concerning cardiac arrest and resuscitation, In CARDIAC ARREST AND RESUSCITATION, CV Mosby Co, St Louis, 1974.
20. Rudikoff MT, Maughan WL, Effron M, Freund P, Weisfeldt ML. Mechanisms of blood flow during cardiopulmonary resuscitation. Circulation 1980; 61:345-352.
21. Chandra NC. Mechanisms of blood flow during CPR. Ann Emerg Med 1993; 22:281-8.
22. Babbs CF. Effects of an impedance threshold valve upon hemodynamics in standard CPR: studies in a refined computational model. Resuscitation 2005; 66:335-345.
23. Posey J, Geddes L. Measurement of the modulus of elasticity of the arterial wall. Cardiovascular Research Center Bulletin 1973; 11:83-103.
24. Brennan EG, O'Hare NJ, Walsh MJ. Transventricular pressure-velocity wave propagation in diastole: adherence to the Moens-Korteweg equation. Physiol Meas 1998; 19:117-23.
25. Callaghan FJ, Babbs CF, Bourland JD, Geddes LA. The relationship between arterial pulse-wave velocity and pulse frequency at different pressures. J Med Eng Technol 1984; 8:15-8.
26. Korteweg DJ. Uber die Fortpflanzungsgeschwindigkeit des Schalles in elastischen Rohren. Ann Phys Chem 1878; 5:525-542.

Table 1: Model parameters for an idealized, 70 kg adult human*

Resistances (>0)

	Value (mmHg/L/sec)	Definition
Rh	5610	Resistance of the head vasculature
Rtv	5	Resistance of the tricuspid valve
Rpv	10	Resistance of the pulmonic valve
Rmv	5	Resistance of the mitral valve
Rav	10	Resistance of the aortic valve
Rpc	120	Resistance of the pulmonary capillaries
Rs	1615	Resistance of truncal systemic vasculature and coronary vessels
Rl	9060	Resistance of leg vasculature
Rairway	1.18	Resistance of airways

Compliances (>0)

	Value (L/mmHg)	Definition
Crh	0.02	Compliance of the arrested right ventricle and pulmonary arteries
Clv	0.02	Compliance of the pulmonary veins, left atrium, and arrested left ventricle
Ccar	0.0002	Compliance of both carotid arteries
Cao	0.0008	Compliance of the thoracic aorta
Caa	0.0004	Compliance of the abdominal aorta
Cfa	0.0002	Compliance of both femoral arteries
Ca_tot	0.0016	Compliance of great arteries
Ca	0.0004	Compliance of aortic segment
Cra	0.0095	Compliance of the right atrium and intrathoracic great veins
Cjug	0.0120	Compliance of both jugular veins
Civc	0.0234	Compliance of the inferior vena cava
Cfv	0.0047	Compliance of both femoral veins
Cv_tot	0.0500	Compliance of great veins
Cv	0.0125	Compliance of caval segment
Clung	0.7400	Lung-chest compliance

Other variables

	Value and units	Definition
Frequency	0.1 to 5 Hz	Number of cycles per second of sinusoidal z-axis motion
Amplitude	1 to 20 cm	Half maximal excursion of periodic z-axis motion equal to the value of B in the expression $\Delta z = B\sin(\omega t)$
ω	0.6 to 30 Hz	Angular frequency equal to 2π times frequency
ΔL	12 cm	Aortocaval segment length
Pinit	10 mmHg	Initial equilibrium pressure of arrested circulation
Pmax	10 – 30 mmHg	Peak pressure for abdominal compression
Pmouth	0 mmHg	Inspiratory gas pressure at the mouth
ρ	1.05 g/ml	Blood density
Δt	0.001 sec	Time step for numerical integration
ν	0.003 Pa-sec	Blood viscosity
T1, T2, T3, T4	1.4, 1.2, 0.8, 0.4	Tapering factors for segmental aortic compliance in simulations of abdominal compression

*Adapted from Babbs[22]

Figures and legends

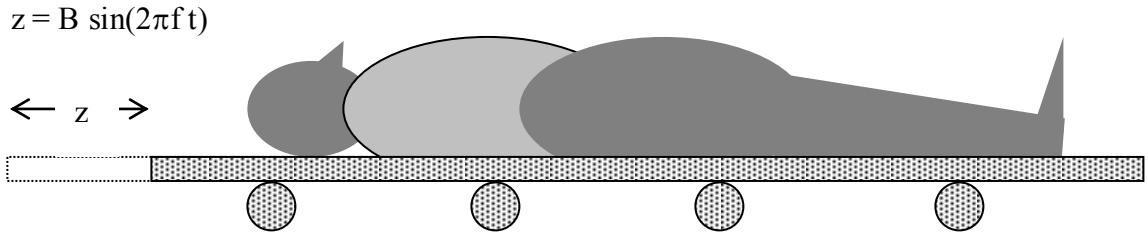

Figure 1: A person on a horizontally oscillating platform. B is the amplitude of oscillation; f is the frequency; t is time. Smooth shading indicates average regional density, which is less in air-filled lungs. Nylon wheels beneath platform allow horizontal oscillating motion.

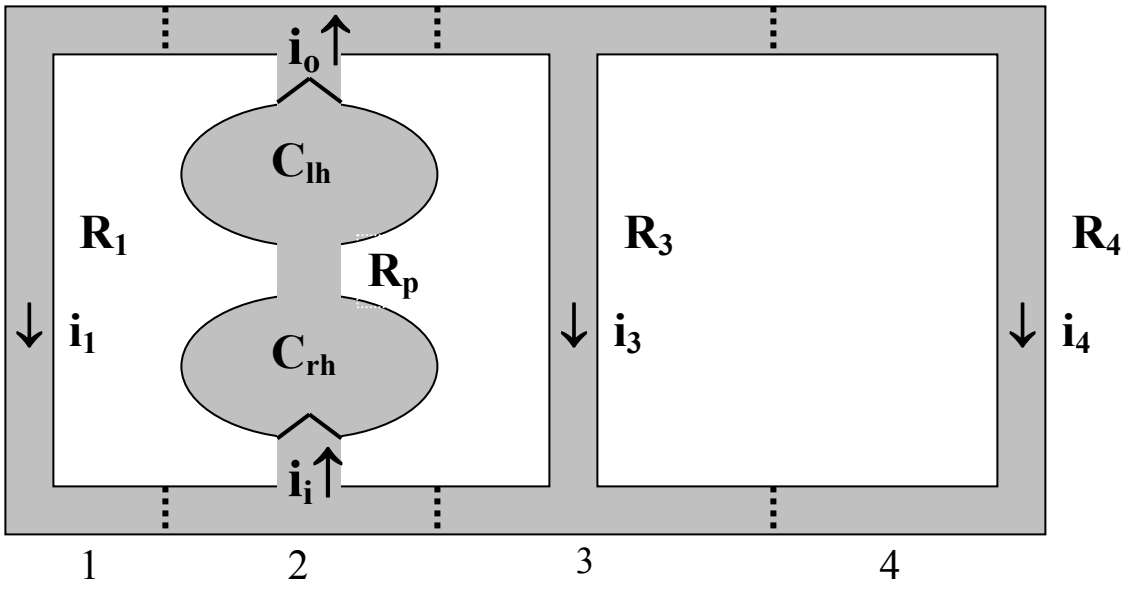

Figure 2: Model of the circulatory system. The aorta (top) and vena cavae (bottom) are divided into matching segments 1, 2, 3, and 4. Segments 1 functionally include carotid arteries and jugular veins. Segments 4 functionally include iliac vessels. Blood flows in a fountain-like pattern upward in section 2 through the pulmonary circulation and downward in sections 1, 3, and 4 through systemic vascular beds. Arrows indicate flows i_i (input to right heart through tricuspid valve), i_o (output from left heart through aortic valve), i_1 (head flow), i_3 (truncal flow), and i_4 (lower extremity flow). R_1, R_p, R_3, and R_4 are vascular resistances of the head, pulmonary vessels, abdomen, and legs respectively. C_{lh} and C_{rh} are lumped left and right heart compliances, including atria, ventricles, pulmonary veins, and pulmonary arteries.

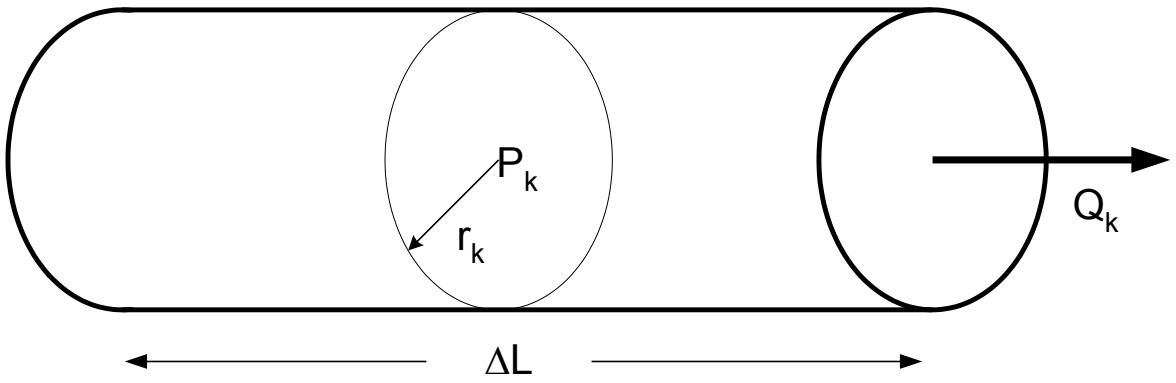

Figure 3: Schematic drawing of aortocaval segment, k, having radius r_k and length ΔL . The pressure at the midpoint is P_k and the flow from the right hand end is Q_k . Segments k = 1, 2, 3, and 4 are connected in a straight line.

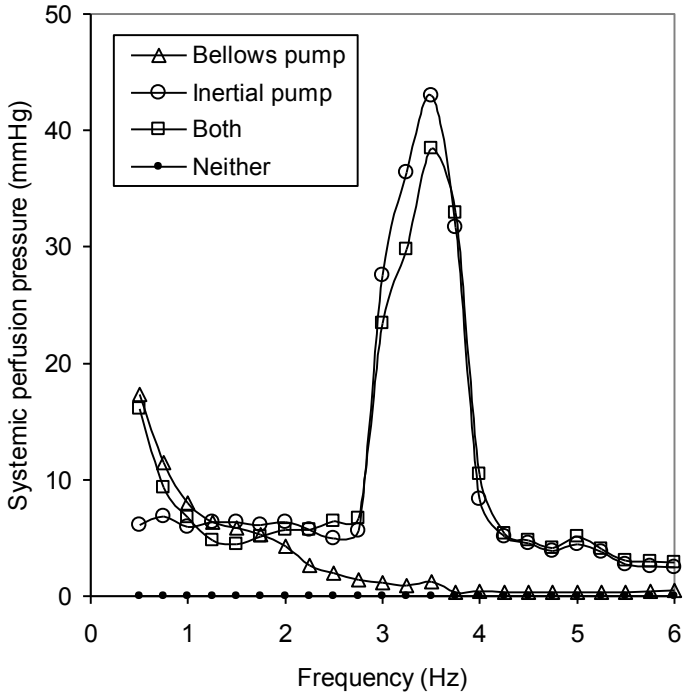

Figure 4(a): Frequency spectrum of systemic perfusion pressure during simulated sinusoidal ± 0.6G pGz-CPR produced by two hypothetical mechanisms. Bellows pump includes motion of diaphragm only with resulting intrathoracic pressure changes. Inertial pump includes axial motion of blood in aorta and vena cavae only with resulting pressure-volume waves. The bellows pump is ineffective at higher frequencies. The inertial pump produces a sharp peak of systemic perfusion at particular frequencies.

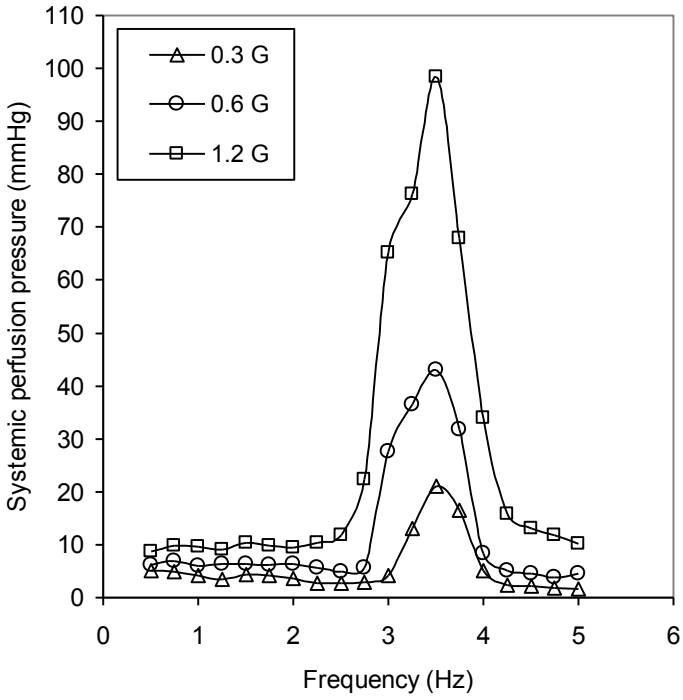

Figure 4(b): Frequency spectra of systemic perfusion pressure during simulated sinusoidal pGz-CPR at different levels of peak acceleration: ± 0.3 G, 0.6 G, and 1.2G. Inertial pump only.

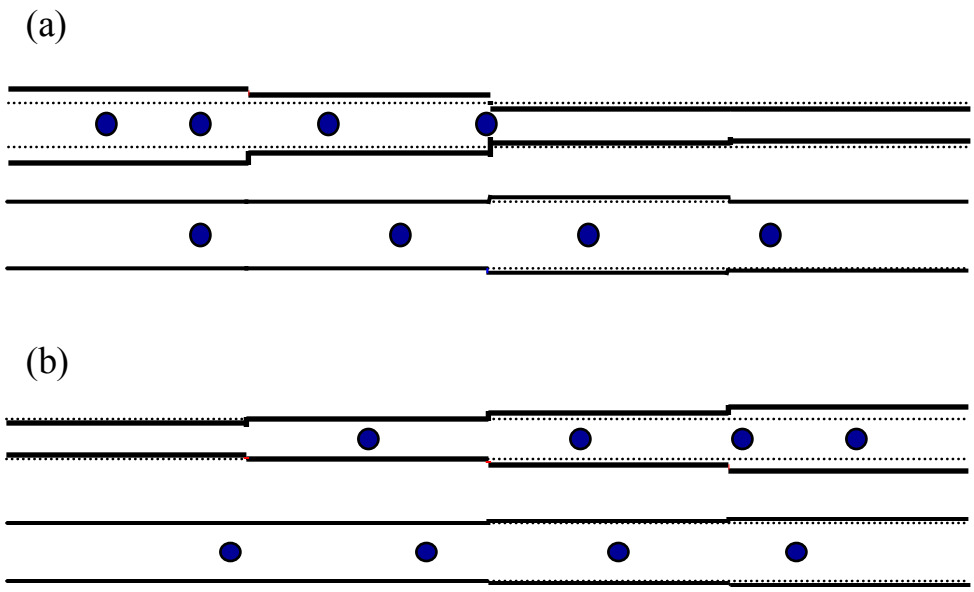

Figure 5: Still frames of graphic animation of blood motion under pGz at peak frequency 3.75 Hz. Peak acceleration ± 0.6 G. Solid lines indicate aortic or caval walls, aortas on top. Dotted lines indicate resting diameters. (a) Freeze frame at 20.051 sec near maximal cranial progress of blood column. (b) Freeze frame at 20.203 sec near maximal caudal progress of blood column. Round balls indicate quintiles of blood volume along the horizontal axis. They can be regarded as suspended markers in the fluid column to aid in visualization of fluid motion.

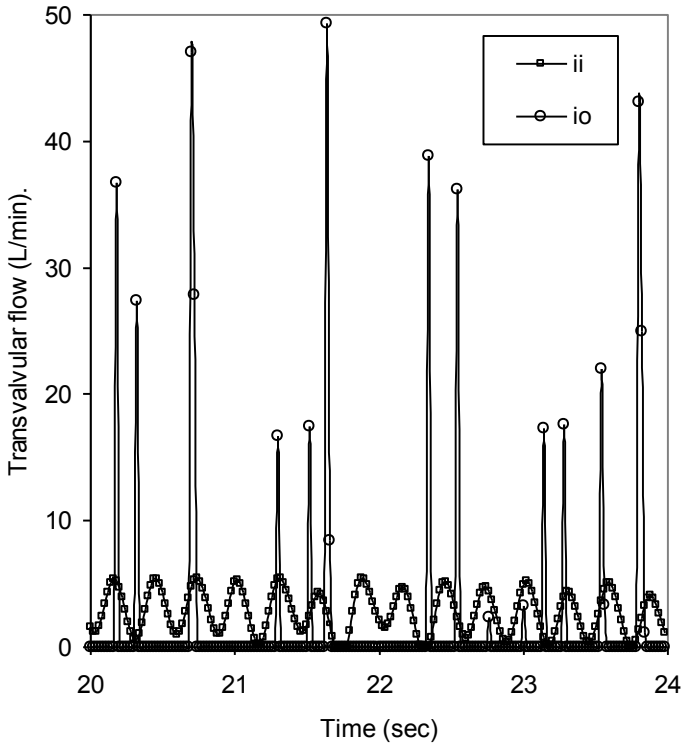

Figure 6: Trans-valvular flows during simulated sinusoidal, ± 0.6G pGz-CPR at peak frequency 3.5 Hz. Details similar to Figure 4. i_i represents inflow across the tricuspid valve. i_o represents outflow across the aortic valve. Trans-aortic flow is intermittent and irregular, occurring in sharp peaks. Inflow is more regular. Both bellows and inertial pump mechanisms are operative.

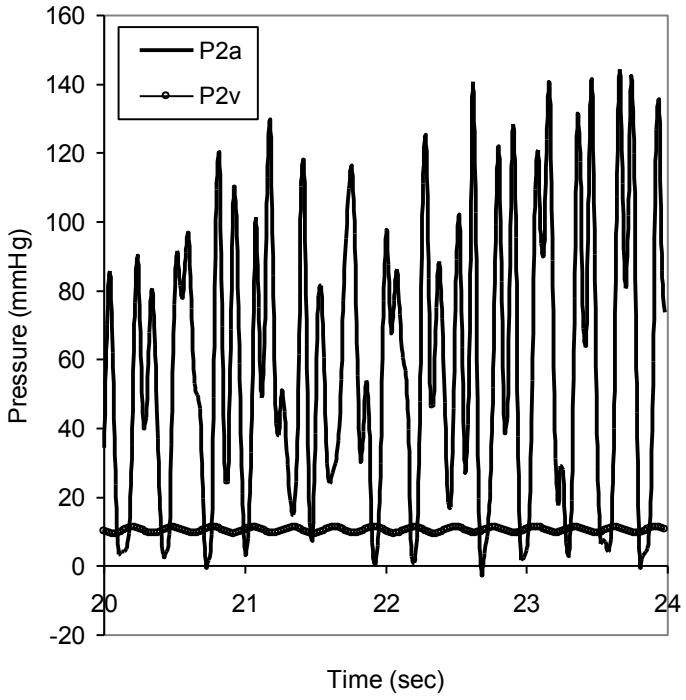

Figure 7(a): Thoracic arterial and central venous pressures during simulated sinusoidal, ± 0.6G pGz-CPR at peak perfusing frequency 3.5 Hz. Details similar to Figure 4. Tall, irregular aortic pressure waves drive systemic perfusion in this idealized adult human model. Both bellows and inertial pump mechanisms are operative.

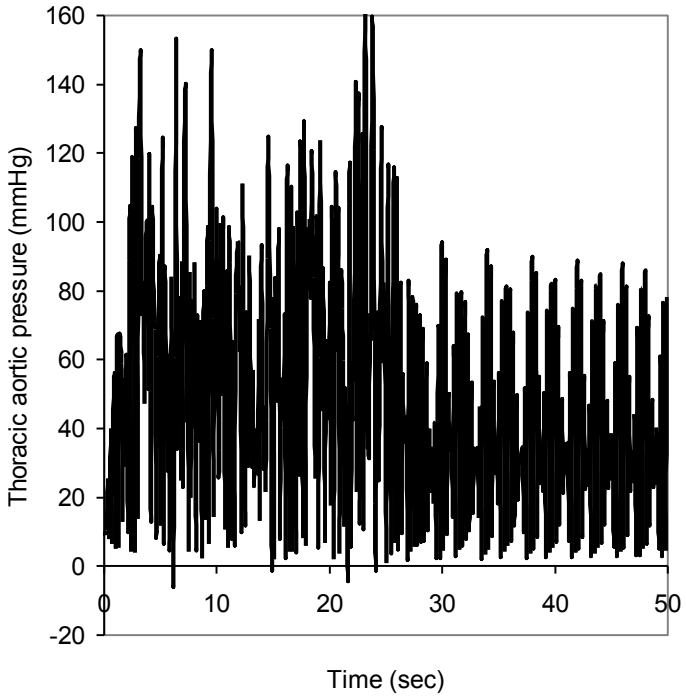

Figure 7(b): Simulation of Figure 7(a) over a continuous 50-second interval at the equivalent of slow chart speed. Initial large amplitude swings in aortic pressure settle into a more regular pattern after 25 seconds of pGz. Central venous pressure (not shown) remains near 10 mmHg.

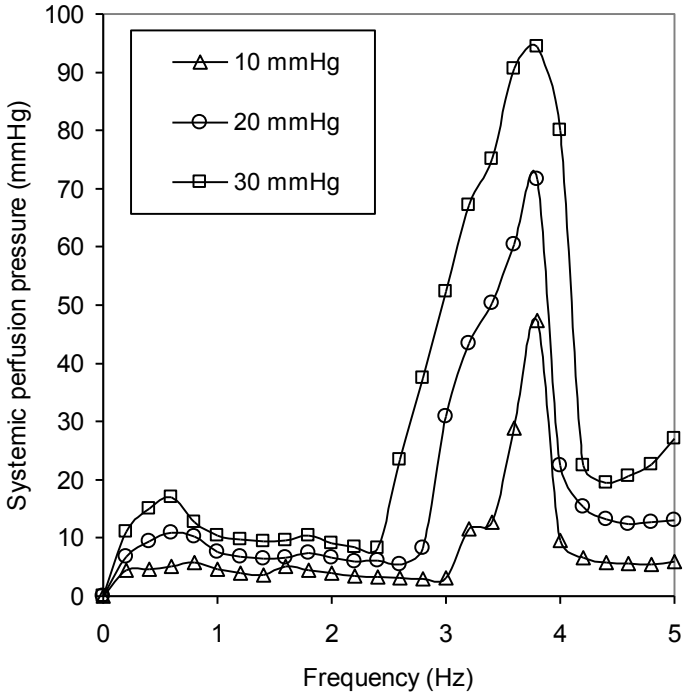

Figure 8: Frequency spectrum of systemic perfusion pressure during simulated inertial pump CPR produced by abdominal compressions ranging from zero to various peak pressures in mmHg. Aortic resonance can be induced by abdominal compression as well as z-axis acceleration. The inertial pump produces sharp peaks of systemic perfusion at particular frequencies. Only modest abdominal pressures are required. In this simulation the aortic compliance was tapered from head to tail in segments 1 through 4 to 160%, 120%, 80%, and 40% of the mean value for the aorta.

Appendix 1: numerical methods

Inertial flows. Let superscripts denote time step indices, and let subscripts indicate the axial positions (1 through 4) of the aortocaval segments illustrated in Figure 2. Let Δt be the time step for numerical integration. We may approximate the derivatives by forward differences, that is, at time step, n, for function y = f(t), we have $dy/dt \cong \left(y^{n+1} - y^n\right)/\Delta t$. Our goal is to compute Q_k^{n+1} for segments k = 1, 2, and 3, given the current values of Q_k^n, the time-varying forcing function, g, and the model parameters. If this is done in a general way, one can start with the initial conditions $Q_k^0 = 0$, etc., and find flows after any number of successive time steps.

Re-writing equation (5b) in terms of the forward difference,

$$\frac{1}{\Delta t}\left(\frac{Q_k^{n+1}}{A_k'^{n+1}} - \frac{Q_k^n}{A_k'^n}\right) = \frac{P_k^n - P_{k+1}^n}{\rho \Delta L} + g \; - \frac{8\pi \nu Q_k^n}{\rho\left(A_k'^n\right)^2} \tag{6a}$$

or

$$\frac{1}{\Delta t}\left(Q_k^{n+1}\frac{A_k'^n}{A_k'^{n+1}} - Q_k^n\right) = A_k'^n\left(\frac{P_k^n - P_{k+1}^n}{\rho \Delta L} + g\right) - \frac{8\pi \nu Q_k^n}{\rho A_k'^n} \tag{6b}$$

Now, solving for Q_k^{n+1} explicitly, and recognizing that for small time steps

$\frac{A_k'^n}{A_k'^{n+1}} \cong 1$, we can write

$$Q_k^{n+1} = Q_k^n\left(1 - \frac{8\pi\nu\Delta t}{\rho A_k'^n}\right) + \frac{\Delta t A_k'^n}{\rho \Delta L}\left(P_k^n - P_{k+1}^n + g\rho\Delta L\right). \tag{6c}$$

Organ blood flows. Equations (6a) through (6c) describe flows caused by z-axis acceleration within each aortocaval segment of the model. We must also describe blood flow through systemic and pulmonary vascular beds, which is governed by viscous forces of vascular resistance. This resistive flow is generally perpendicular to the z-axis and determined by arteriovenous pressure differences. Using the double subscripts 1a, 1v, 2a, 2v, etc. to indicate the aortic and venous (caval) segments 1, 2, 3, and 4, the resistive flows in the model at any instant in time are

$i_1 = \left(P_{1a} - P_{1v}\right)/R_1$
$i_3 = \left(P_{3a} - P_{3v}\right)/R_3$

$$
\begin{aligned}
i_4 &= \left(P_{4a} - P_{4v}\right)/R_4 \\
i_i &= \max\left(0, \left(P_{2v} - P_{rh}\right)/R_{tv}\right) \\
i_p &= \left(P_{rh} - P_{lh}\right)/R_p \\
i_o &= \max\left(0, \left(P_{lh} - P_{2a}\right)/R_{av}\right) .
\end{aligned} \tag{7}
$$

Here the max() function is used to represent the one-way flow inflow, i_i , and outflow, i_o , produced by competent heart valves. The small in-line resistances R_{tv} and R_{av} are those provided by the tricuspid and aortic valves.

Collapse of aortocaval segments. Periodic z-axis acceleration or vigorous external compression tends to shift blood rapidly along the longitudinal axes of the aorta and vena cavae from one end to the other. Aortocaval segments in the trailing portions of the fluid wave become partially emptied and tend to collapse toward zero volume. Negative volumes in these segments are not allowed. In the numerical methods it is necessary to deal with potential collapsed segments gracefully. The physical principle involved is that blood can flow into a collapsed segment from either end or from a side branch; however, blood cannot flow out of a collapsed segment from either end or from a side branch. Consider, for example, aortic segment 1, denoted segment 1a, which began the simulation with initial volume V_{0a}. If its present volume V_{1a} is essentially zero, that is if $V_{1a}/V_{0a} < \varepsilon$ for some small positive $\varepsilon << 1$ (here we use $\varepsilon = 0.1$), then if the previously calculated value of Q_{1a} is positive (leaving segment 1) then we must set $Q_{1a} = 0$. Also, if the previously calculated head blood flow, i_1 is positive (leaving segment 1) then we must set $i_1 = 0$ during the collapsed state. However, inflow to segment 1a must be allowed, or else it will remain permanently collapsed, which would be unrealistic. Similarly, if the volume of segment 2v (right atrium) becomes very small, then positive values of Q_{2v} and positive values of right heart inflow, i_i , are not allowed. Negative values of Q_{1v}, indicating outflow from segment 2v, also are not allowed. In this fashion, logical tests were performed for collapse of each aortocaval segment, in turn, and any outflows from a collapsed segment were set to zero to avoid creating physically unrealistic negative volumes.

Aortocaval volumes. Knowing both inertial and resistive flows at each time step Δt, we can update the aortocaval segment volumes thus:

$$
\begin{aligned}
V_{1a}^{n+1} &= V_{1a}^{n} + \left(-Q_{1a}^{n} - i_1\right)\Delta t \\
V_{2a}^{n+1} &= V_{2a}^{n} + \left(Q_{1a}^{n} - Q_{2a}^{n} + i_o\right)\Delta t \\
V_{3a}^{n+1} &= V_{3a}^{n} + \left(Q_{2a}^{n} - Q_{3a}^{n} - i_3\right)\Delta t \\
V_{4a}^{n+1} &= V_{4a}^{n} + \left(Q_{3a}^{n} - i_4\right)\Delta t
\end{aligned} \tag{8}
$$

and

$$
\begin{aligned}
V_{1v}^{n+1} &= V_{1v}^{n} + \left(-Q_{1v}^{n} + i_1\right)\Delta t \\
V_{2v}^{n+1} &= V_{2v}^{n} + \left(Q_{1v}^{n} - Q_{2v}^{n} - i_i\right)\Delta t
\end{aligned}
$$

$$V_{3v}^{n+1} = V_{3v}^{n} + \left(Q_{2v}^{n} - Q_{3v}^{n} + i_3\right)\Delta t$$
$$V_{4v}^{n+1} = V_{4v}^{n} + \left(Q_{3v}^{n} + i_4\right)\Delta t\,. \qquad (9)$$

The algebraic signs in (8) and (9) are easily understood with reference to Figure 2. At this juncture it is numerically prudent to test for conservation of volume in the entire model. This was done by computing the aggregate volume change $\Delta V_{tot} = \sum_k C_k\left(P_k - P_0 - P_{ext}\right)$ for all 10 vascular compartments, k, including the left and right heart compartments. For the thoracic aortocaval segments 2a and 2v the external pressure P_{ext} is equal to the intrathoracic pressure, P_{lung}. For simulations of active abdominal pressure P_{ext} is the forcing pressure felt by the abdominal aortocaval segments. In the simulations reported here ΔV_{tot} was always much less than 1 microliter or a tiny drop of blood. Volume conservation was always achieved.

Remaining variables. In turn, the segmental cross-sectional areas are found as

$$A_k^{n+1} = V_k^{n+1`}/\Delta L \qquad (10)$$

for k = 1, 2, 3, and 4 in arteries and veins. Then updated segmental pressure values are found from the pressure-volume relationship

$$P_k^{n+1} = P_k^0 + \frac{V_k^{n+1} - V_k^0}{C_k}. \qquad (11)$$

Here the vascular walls are treated as simple compliances. Similarly, pressures in the right and left heart compliances are updated at each time step as

$$P_{rh}^{n+1} = P_{rh}^{n} + dP_{lung} + \frac{\left(i_i^n - i_p^n\right)\Delta t}{C_{rh}} \quad \text{and} \quad P_{lh}^{n+1} = P_{lh}^{n} + dP_{lung} + \frac{\left(i_p^n - i_o^n\right)\Delta t}{C_{lh}}, \qquad (12)$$

where dP_{lung} comes from Equation (3) describing the counterbalancing effects of phrenic motion toward the head and gas outflow from the trachea. In this way it is possible to calculate numerically the pressures, volumes, and flows in all compartments of the model.

Appendix 2: predicting aortic resonant frequency

For a thin walled elastic tube of initial radius r_0, expanded radius $r = r_0 + \Delta r$, length L, wall thickness, h, and Young's modulus of elasticity, E, the resting un-stretched compliance, as derived for example in reference[23], is

$$C = \frac{2\pi L r_0^3}{Eh} \text{ or equivalently } Eh = \frac{2\pi L r_0^3}{C}.$$

Here we regard L as the total aortic length and C as the total aortic compliance. Using the classical Moens-Korteweg equation[24-26], we can express pulse wave speed, s, along the tube with cross sectional area $A = \pi r^2$, in terms of model parameters thus:

$$s = \sqrt{\frac{Eh}{2\rho(r_0 + \Delta r)}} = \sqrt{\frac{2\pi L r_0^3}{2C\rho(r_0 + \Delta r)}} = \sqrt{\frac{LA_0}{C\rho(1 + \Delta r / r_0)}}.$$

For a tube with closed ends the round-trip transit time for a reflected pulse wave is

$$t_{rt} = \frac{2L}{s} = 2L\sqrt{\frac{C\rho(1 + \Delta r / r_0)}{LA_0}} = 2\sqrt{\frac{LC\rho(1 + \Delta r / r_0)}{A_0}},$$

and the resonant frequency would be

$$f^* = \frac{1}{t_{rt}} = \frac{1}{2}\sqrt{\frac{A_0}{LC\rho(1 + \Delta r / r_0)}}.$$